

NUMERICAL SIMULATION OF OPTICAL CHARACTERISTICS OF SPHERICAL PARTICLES POLYDISPERSIONS

A.V. Vasil'ev and L.S. Ivlev

*Scientific—Research Institute of Physics
at the St. Petersburg State University
Received October 21, 1994*

Numerical simulation of the total and differential scattering cross sections of homogeneous spherical particles polydispersions with different particle size distribution functions within a wide range of the complex refractive index at 550 nm wavelength was performed. The differential scattering cross sections have been studied as a function of a complex refractive index.

Microphysical aerosol models used in calculating the characteristics of radiation field in the atmosphere (particle number density, particle size distribution, and complex refractive index of aerosol substance) are of practical importance due to their completeness and possible derivation of the required optical characteristics in a wide spectral range. Nevertheless they exhibit some serious disadvantages because they need for a large number of parameters which depend on the nature of aerosol particles, on the time and conditions of the particles staying in the atmosphere (meteorological factors).^{1–3}

In some cases, in particular in the visible spectral range, the empirical formulas and relations for optical characteristics of atmospheric aerosols depending on different meteorological factors and types of air mass which adequately describe real situations were obtained in Refs. 4 and 5. This is mainly caused by a small spread of microstructural parameters in aerosol systems, their averaging in large air volumes, and the governing effect of some meteorological factors and processes, in particular, relative humidity, on the aerosol structure.^{6–8}

Quantitatively important variations of optical aerosol characteristics, transitions from one type of their optical properties to the others can be accounted for by a phase transition (variation in particle shape), variation of chemical composition of aerosol substance (the complex refractive index), and noticeable growth of particles (condensation growth at high relative humidity). We restrict our consideration by the case of polydisperse systems of homogeneous spherical particles and consider transformation of the scattering phase function for possible changes in disperse and chemical composition of aerosol particles. The calculations were made for a single mode distribution described by different analytical expressions.

In the calculations we use the effective parameters of the particle size distribution functions, namely, the effective radius r_{eff} and effective width of the distribution V_{eff} :

$$r_{\text{eff}} = M_3/M_2; V_{\text{eff}} = M_2 M_4/M_3^2 - 1; M_i = \int_0^{\infty} r^i f(r) dr, \quad (1)$$

where $f(r)$ is the normalized particle size distribution function. As shown in Ref. 9, the optical characteristics of clusters of aerosol particles described by different distribution functions with equal effective parameters weakly depend on the specific form of the distribution function. Therefore in the calculations a set of values of

r_{eff} and V_{eff} was used as unified parameters of the aerosol particle size distribution functions.

The calculations were made for values of V_{eff} equal to 0.1, 0.25, 0.5, 1, 2.5 and r_{eff} equal to 0.05, 0.1, 0.5, 1, 2.5, 5, and 10 μm .

In the calculations the four distribution functions were used.

1. Lognormal distribution (two parameters, r_0 and σ):

$$f(r) = (C/r) \exp(-\ln^2(r/r_0)/2\sigma^2), \quad (2)$$

for which

$$r_{\text{eff}} = r_0 \exp(2.5\sigma^2) \text{ and } V_{\text{eff}} = \exp(\sigma^2) - 1. \quad (3)$$

Hence,

$$\sigma = \sqrt{\ln(V_{\text{eff}} + 1)}; \quad r_0 = r_{\text{eff}} / \exp(2.5\sigma^2). \quad (4)$$

2. Gamma distribution (two parameters, $\alpha > 1$ and β):

$$f(r) = C r^{\alpha-1} \exp(-r/\beta). \quad (5)$$

For which

$$r_{\text{eff}} = (\alpha + 2)\beta; V_{\text{eff}} = (\alpha + 3)/(\alpha + 2) - 1. \quad (6)$$

Hence,

$$\alpha = \frac{1}{V_{\text{eff}}} - 2; \beta = r_{\text{eff}} / (\alpha + 2). \quad (7)$$

It follows from the condition $\alpha > 1$ that V_{eff} for the gamma distribution cannot exceed 0.333.

3. Junge distribution (two parameters, r_1 and β):

$$f(r) = \begin{cases} C, & \text{if } r < r_1, \\ C(r/r_1)^{-\beta}, & \text{if } r \geq r_1. \end{cases} \quad (8)$$

The parameters r_1 and β for the given values V_{eff} and r_{eff} were calculated for the Junge distribution by the trial-and-error method.

4. Inverse gamma distribution (two parameters, $\alpha > 1$ and β):

$$f(r) = C r^{1-\alpha} e^{-\beta/r}. \quad (9)$$

The parameters α and β for the given values V_{eff} and r_{eff} were calculated for the inverse gamma distribution by the trial-and-error method too.

The values of distribution parameters corresponding to the given effective ones are listed in the table.

For all of the aforementioned distribution functions and a set of parameters we calculated the total and differential scattering cross sections at the radiation wavelength of 0.55 μm , a real part of the refractive index of 1.33, 1.40, 1.45, 1.50, 1.60, 1.65, 1.80, and 2.20, and an imaginary part of the refractive index of 0, 0.0005, 0.001, 0.005, 0.01, 0.03, 0.05, and 0.1. A given set of refractive indices almost fully covers the range of possible variation of the aerosol substance refractive index. The differential scattering cross sections were calculated for the scattering angles 0–20° with the 5° step,

30–170° with the 10° step, and 175, 180° (altogether there were 22 angles).

The calculational results supported the two known conclusions^{4,9}: 1) the total scattering cross sections and the differential scattering cross sections only slightly depend on the specific form of the particle size distribution function but depend on the effective parameters of distribution (r_{eff} and V_{eff}); 2) the connection between the differential scattering cross section and the total scattering cross section is well approximated by the linearly–logarithmic relation

$$\log S(\gamma) = A(\gamma) + B(\gamma) \log \sigma, \tag{10}$$

where $S(\gamma)$ is the differential scattering cross section for the angle γ , and σ is the total scattering cross section.

TABLE I. Values of parameters of particle size distribution functions.

V_{eff}	r_{eff}	Distribution							
		Lognormal		Gamma		Junge		Inverse gamma	
		r_0	σ	α	β	r_1	β	α	β
0.1	0.05	0.039	0.309	8	0.005	0.0565	9.6	16	0.5
	0.1	0.079	0.309	8	0.01	0.113	9.7	16	1.1
	0.5	0.394	0.309	8	0.05	0.56	9.6	16	5.5
	1	0.788	0.309	8	0.1	1.139	9.7	16	11
	2.5	1.969	0.309	8	0.25	2.82	9.67	16	27
	5	3.938	0.309	8	0.5	5.65	9.61	16	55
	10	7.876	0.309	8	1	11.3	9.7	16	110
0.25	0.05	0.0286	0.472	2	0.0125	0.048	6.62	10	0.2
	0.1	0.0573	0.472	2	0.025	0.097	6.62	10	0.5
	0.5	0.286	0.472	2	0.125	0.48	6.62	10	2.5
	1	0.573	0.472	2	0.25	0.965	6.62	10	5
	2.5	1.432	0.472	2	0.625	2.41	6.62	10	12
	5	2.865	0.472	2	1.25	4.82	6.61	10	25
	10	5.729	0.472	2	2.5	9.64	6.61	10	50
0.5	0.05	0.018	0.637			0.043	5.86	8	0.15
	0.1	0.0363	0.637			0.087	5.86	8	0.30
	0.5	0.181	0.637			0.43	5.86	8	1.5
	1	0.363	0.637			0.867	5.86	8	3
	2.5	0.907	0.637			2.16	5.85	8	7.5
	5	1.813	0.637			4.33	5.85	8	15
	10	3.626	0.637			8.62	5.82	8	30
1	0.05	0.00882	0.833			0.0397	5.46	7	0.1
	0.1	0.0176	0.833			0.079	5.45	7	0.2
	0.5	0.088	0.833			0.393	5.44	7	1
	1	0.176	0.833			0.785	5.43	7	2
	2.5	0.441	0.833			1.95	5.41	6.99	4.98
	5	0.882	0.833			3.86	5.38	6.97	9.85
	10	1.764	0.833			7.62	5.33	6.97	19.7
2.5	0.05	0.00219	1.119			0.0357	5.146	6.385	0.069
	0.1	0.00437	1.119			0.071	5.134	6.379	0.138
	0.5	0.022	1.119			0.348	5.093	6.356	0.678
	1	0.044	1.119			0.688	5.064	6.377	1.34
	2.5	0.109	1.119			1.675	5.009	6.297	3.24
	5	0.219	1.119			3.25	4.945	6.246	6.24
	10	0.437	1.119			6.18	4.847	6.159	11.7

The aerosol scattering cross section $\sigma(0.55)$ can be derived from measurement data on meteorological visual range. Concrete form of the aerosol particle size distribution function is usually unknown in the experiments. However based on the first conclusion it is

possible to combine all the distribution functions when constructing the dependence (10). Thus we have constructed the dependence (10) for all of the 128 points given in the table. An example of the dependence (10) for $\gamma = 30$ and 120° is given in Fig. 1.

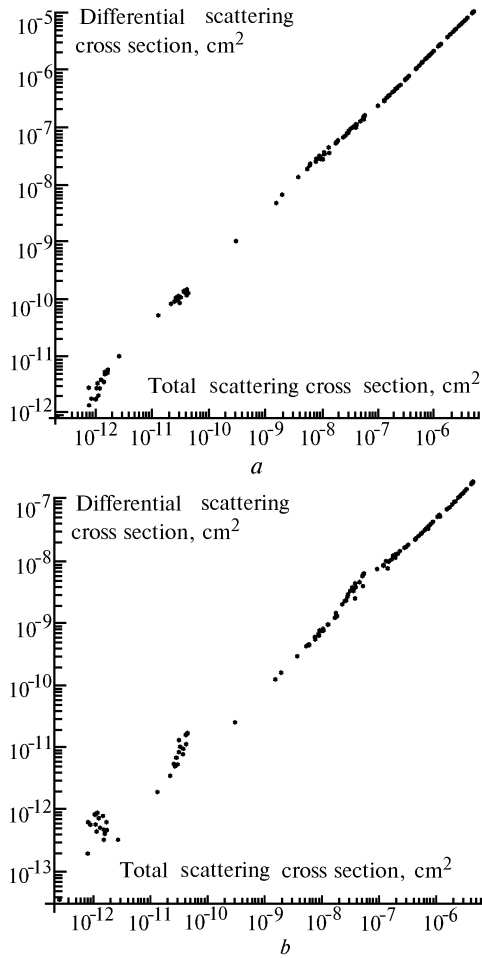


FIG. 1. The differential scattering cross section vs. total scattering cross section. The real part of the refractive index $n = 1.33$, and the imaginary one $\kappa = 0$; the scattering angle $\gamma = 30^\circ(a)$ and $120^\circ(b)$.

It is seen from the figure that a concrete analytical form of the particle size distribution function is not so important for $\sigma(0.55) \geq 10^{-11} \text{cm}^2$, while for $\sigma(0.55) < 10^{-11} \text{cm}^2$ there is observed a dependence on the form of the distribution function. However, it should be noted that this region is related to not very interesting case of a cluster of very small optically inactive particles.

The dependence of the coefficients $A(\gamma)$ and $B(\gamma)$ from Eq. (10) on the complex refractive index (CRI) has been investigated. This dependence was complicated and had a different form at different angles, i.e., we observed transformation of the form of the scattering phase function with variation of the complex refractive index. It should also be noted that the dependences $A(\gamma)$ and $B(\gamma)$ on the complex refractive index turned out to be practically identical. Therefore depicted in Figs. 2–4 are only the examples of the dependence $A(\gamma)$ on the real and imaginary parts of the refractive index.

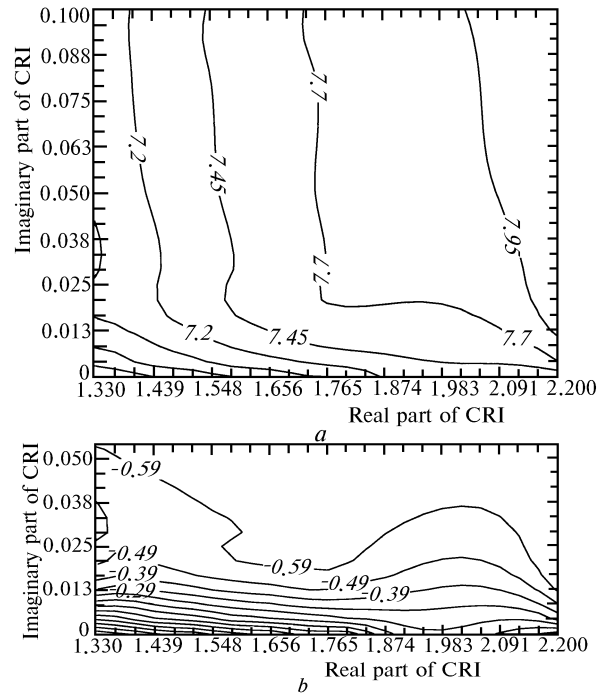


FIG. 2. A plot of the coefficient $A(\gamma)$ vs. the complex refractive index; the scattering angle $\gamma = 0^\circ(a)$ and $20^\circ(b)$.

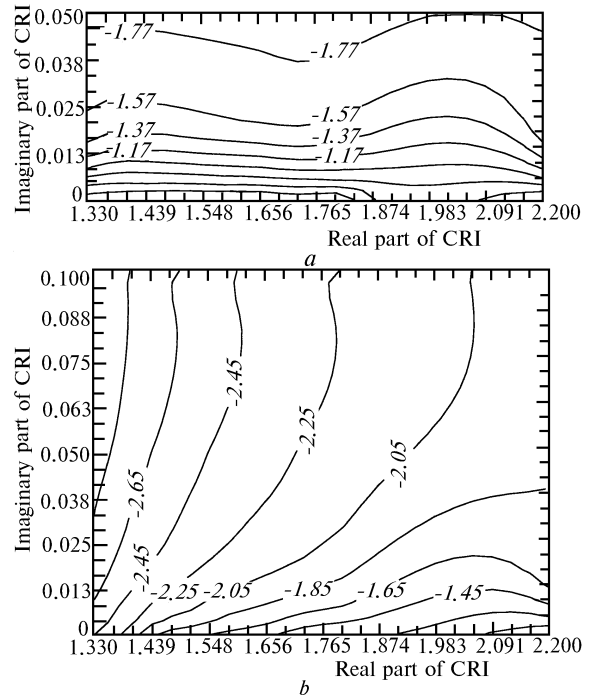


FIG. 3. A plot of the coefficient $A(\gamma)$ vs. the complex refractive index; the scattering angle $\gamma = 40^\circ(a)$ and $90^\circ(b)$.

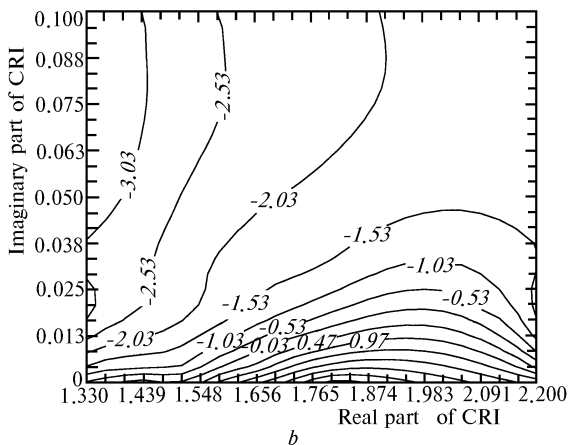
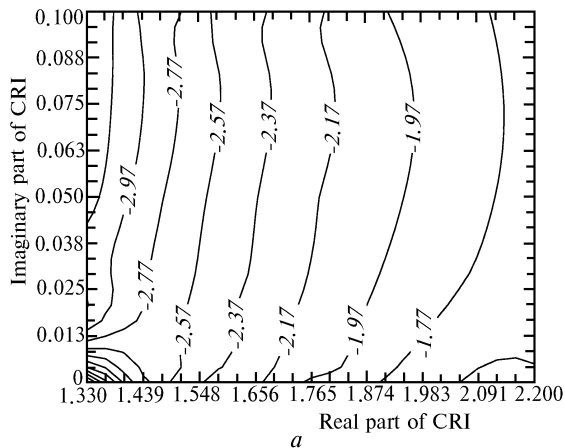


FIG. 4. A plot of the coefficient $A(\gamma)$ vs. the complex refractive index; the scattering angle $\gamma = 140^\circ$ (a) and 180° (b).

There are several regions of different dependences $A(\gamma)$ and $B(\gamma)$ on the complex refractive index of the aerosol substance: 1) a region near $n = 1.33$ with small values of the imaginary part of the refractive index ($\kappa < 0.01$), 2) a region with the imaginary part of the refractive index $n > 1.70$, and 3) the region with the imaginary part of the refractive index $\kappa \geq 0.025-0.030$.

In a real not so polluted atmosphere an effective value of the imaginary part of the refractive index only rarely exceeds $\kappa = 0.01$ and the real part varies within the range between 1.33 and 1.65. Therefore the behaviors of $A(n, \kappa, \gamma)$ and $B(n, \kappa, \gamma)$ were studied at length in the range of $n = 1.33 - 1.65$ and $\kappa = 0 - 0.03$. Some results of calculating $A(n, \kappa)$ at different scattering angles γ are given in Figs. 5 and 6. For angles of $30-60^\circ$ practically no dependence on n is observed, and in the range of angles $70-110^\circ$ and $165-180^\circ$ the increase in n leads to increase in the coefficient $A(n, \kappa)$. At small angles, $\gamma = 0 - 20^\circ$, the increase in n results in a decrease in $A(n, \kappa)$. At angles $120-140^\circ$ when $n > 1.45$ the value $A(n, \kappa)$ is almost constant independent of κ values, and there appear regions of anomalous behavior of $A(n, \kappa)$ (change of behavior) at angles $100-160^\circ$.

These peculiarities in the behavior of the scattering phase function can be used in the solution of inverse problems of aerosol optics. They must be correlated with the empirically found types (classes) of optical weather and types of the scattering phase functions.

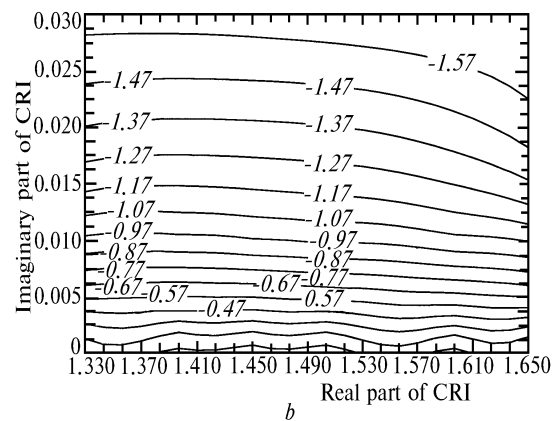
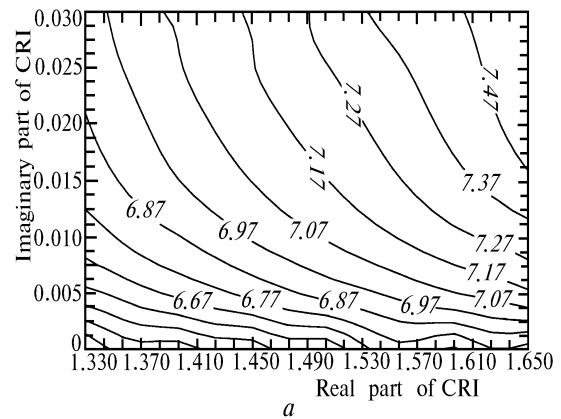


FIG. 5. A plot of the coefficient $A(\gamma)$ vs. the complex refractive index in the range $n = 1.33-1.65$; $\kappa = 0-0.03$; the scattering angle $\gamma = 0^\circ$ (a) and 40° (b).

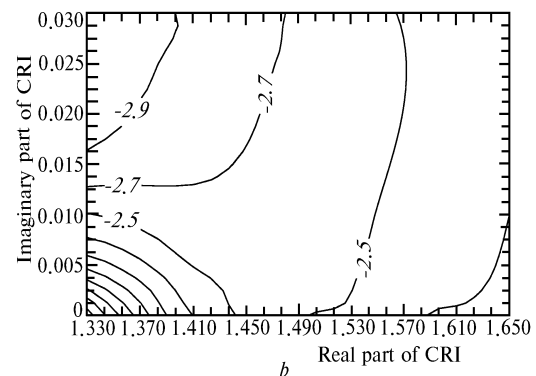
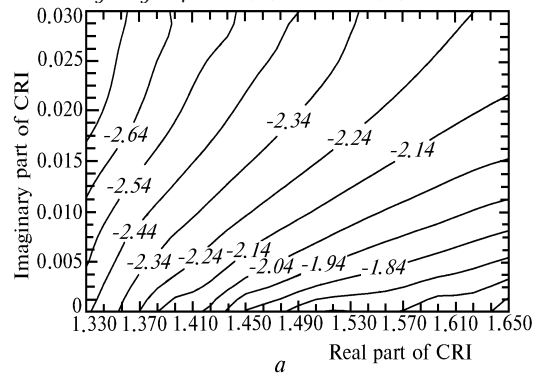


FIG. 6. A plot of the coefficient $A(\gamma)$ vs. the complex refractive index in the range $n = 1.33-1.65$; $\kappa = 0-0.03$; the scattering angle $\gamma = 90^\circ$ (a) and 140° (b).

The general regularities in variation of the behavior of the scattering phase functions at one wavelength or integrated over visible spectrum are accounted for by optical thickness of polydisperse aerosol (relation between the coefficients of aerosol and molecular scattering) and the value of the complex refractive index. The shape of the integral scattering phase function does not bear any information about whether the particle size distribution is unimodal or polymodal. A more complete information on aerosol particle size distribution may be extracted from measurements of the scattering phase function at different wavelengths.

An important fact is the absence of noticeable dependence of $A(n, \kappa)$ on n in the range of scattering angles $\gamma = 30\text{--}60^\circ$ (Refs. 10 and 11) for which the relation

$$\sigma = \text{const } S(30\text{--}60^\circ) \quad (11)$$

holds.

On the one hand, all the aforesaid enables one to simulate, simply and with a satisfactory accuracy, a set of optical characteristics of atmospheric aerosols (coefficients of total and differential scattering, scattering phase functions, and optical thickness) based on incomplete experimental optical or microphysical data.

On the other hand, it is clear that the data on scattering phase function at a single wavelength are inadequate to solve the inverse problems of aerosol optics. We also have to have the data on spectral behavior of the scattering coefficient and the complex refractive index of aerosol substance. In this case it is possible to distinguish not more than 3 to 4 modes.

To find the solution, it is convenient to use *a priori* distribution functions for different modes and the obtained array of data for r_{eff} , V_{eff} , n , and κ . The use of empirical

relationships between the optical and microphysical parameters of aerosols is difficult in this case.

REFERENCES

1. K.Ya. Kondrat'ev, ed., *Aerosol and Climate* (Gidrometeoizdat, Leningrad, 1991), 541 pp.
2. V.E. Zuev and G.M. Krekov, *Optical Models of the Atmosphere* (Gidrometeoizdat, Leningrad, 1986), 256 pp.
3. L.S. Ivlev and S.D. Andreev, *Optical Properties of Atmospheric Aerosols* (State University, Leningrad, 1986), 358 pp.
4. G.I. Gorchakov and M.A. Sviridenkov, *Izv. Akad. Nauk SSSR, Fiz. Atmos. Okeana* **15**, No. 1, 53–59 (1979).
5. O.D. Barteneva, E.N. Dovgiallo, and E.A. Polyakova, *Tr. Gl. Geofiz. Obs.*, No. 220, 224 (1967).
6. G.V. Rozenberg, G.I. Gorchakov, Yu.S. Georgievskii, and Yu.S. Lyubimtseva, in: *Physics of the Atmosphere and Problems of Climate* (Nauka, Moscow, 1980), pp. 236–249.
7. L.S. Ivlev, *Chemical Composition and Structure of Atmospheric Aerosols* (State University, Leningrad, 1982), 368 pp.
8. G.Sh. Livshits, A.N. Solov'eva, and T.B. Travina, *Izv. Akad. Nauk SSSR, Fiz. Atmos. Okeana* **10**, No. 8, 991–993 (1974).
9. N.L. Lukashevich and V.P. Shari, in: *Numerical Solution of Problems of Atmospheric Optics* (M.V. Keldysh Institute of Applied Mathematics, Moscow, 1984), pp. 199–211.
10. E.V. Pyaskovskaya–Fesenkova, *Investigation into the Light Scattering in the Earth's Atmosphere* (USSR Academy of Sciences, Moscow, 1957), 218 pp.
11. K.S. Shifrin and E.A. Chayanova, *Izv. Akad. Nauk SSSR, Fiz. Atmos. Okeana* **3**, No. 3, 274–283 (1967).